Supplementary Information (SI) for RSC Advances.
This journal is © The Royal Society of Chemistry 2026

Supplementary Information

Construction of a Cu/Fe/S Multi-Active-Site Synergistic Fenton-like System via Mechanically Activated Natural Copper Sulfide Ore for Efficient Tetracycline Degradation

Lizheng Gou[a,b,c], Xiwang Miao[c], Yuhang Liu [a,b], Mei Zhang[a,b], Min Guo[a,b,*]

[a]*State Key Laboratory of Advanced Metallurgy, School of Metallurgical and Ecological Engineering, University of Science and Technology Beijing, Beijing 100083, P. R. China*

[b]*School of Metallurgical and Ecological Engineering, University of Science and Technology Beijing, Beijing 100083, China*

[C]*MCC CISDI Group Co., Ltd. Chongqing 400013, P. R. China*

Section S1: Full ESR Acquisition Parameters

ESR spectra were recorded on a Bruker A300 spectrometer at room temperature. Acquisition parameters: microwave frequency = 9.85 GHz, microwave power = 20 mW, modulation frequency = 100 kHz, modulation amplitude = 1.0 G, sweep width = 100 G, time constant = 40 ms, sweep time = 60 s. Spin traps: DMPO (5,5-dimethyl-1-pyrroline N-oxide) for ·OH and $\cdot O_2^-$ (50 mM in water), and TEMP (2,2,6,6-tetramethylpiperidine) for $^1O_2$ (50 mM in water). Spectra were recorded immediately after mixing (within 2 min) to capture short-lived radicals.

Section S2: XPS Fitting Parameters

XPS spectra were acquired using an AXIS ULTRA-DLD spectrometer (Kratos Analytical) with monochromatic Al Kα radiation (hν = 1486.6 eV) at 150 W. The pass energy was 40 eV for high-resolution scans. Charge compensation was achieved using

*Corresponding author: Tel/fax: +86 10 62334926, E-mail address: guomin@ustb.edu.cn

a low-energy electron flood gun. All spectra were calibrated to the C 1s peak of adventitious carbon at 284.8 eV.

Peak fitting was performed using Casa XPS software (version 2.3.25). A Shirley background was applied to all spectra. Peaks were modeled using a Gaussian–Lorentzian (GL30) line shape. The following constraints were applied during fitting:

For Fe $2p_{3/2}$: The Fe^{2+} and Fe^{3+} components were allowed to vary in position (±0.2 eV) and FWHM (±0.1 eV) but constrained to have the same FWHM within each oxidation state.

For Cu $2p_{3/2}$: The Cu^{+} and Cu^{2+} peaks were fitted with FWHM constrained to 1.2–1.5 eV and 2.5–3.5 eV, respectively, to account for the broader nature of Cu^{2+} due to multiplet splitting.

For S 2p: The S $2p_{3/2}$ and S $2p_{1/2}$ doublets were constrained with a fixed area ratio of 2:1 and a spin-orbit splitting of 1.18 eV.

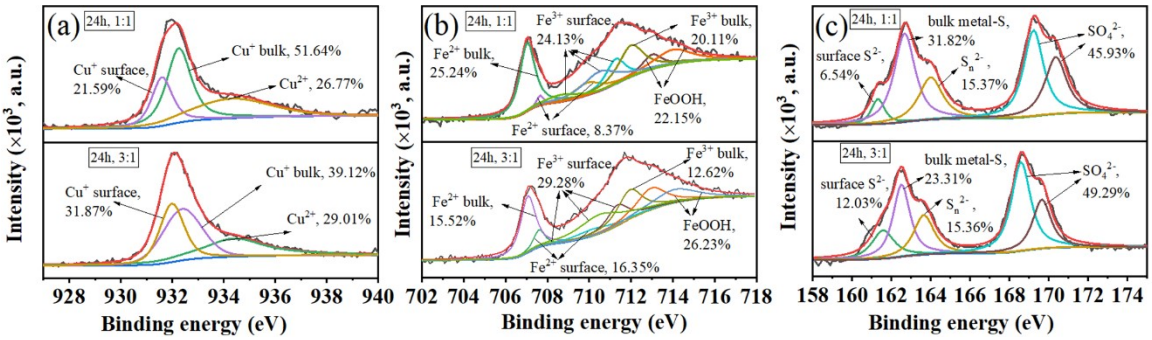

Fig. S1 XPS spectra of catalysts obtained under different ball to material ratios: (a) Cu, (b) Fe, and (c) S.

Section S3: Photocatalytic Experimental Details

Lamp type and specifications (Xe arc lamp, CEL-HXF300, China),

Cutoff filter details (420 nm long-pass),

Light intensity measurement method (radiometer, CEL-NP2000),

Photon flux determination by ferrioxalate actinometry.

Table S1. Comparison of Catalytic Performance with Recent Fenton-Like Catalysts for Antibiotic Degradation.

Catalyst	Pollutant	Conditions	Efficiency	Time	ROS	Ref.
This work	Tetracycline	0.5 g/L, 3 mM H_2O_2, pH 6.2	90.1%	10 min	·OH, $·O_2^-$	–
Synthesized $CuFeS_2$	Tetracycline	0.2 g/L, 5 mM H_2O_2, pH 3.0	99.1%	40 min	·OH	[1]
Synthesized FeS_2	Tetracycline	0.05 g/L, 1 mM PMS, pH 5.6	91%	60 min	·OH, $·SO_4^{2-}$	[2]
Synthesized $CuFeS_2$@ FeS_2	Tetracycline	0.2 g/L, 0.2 g/L PMS, pH 3	91.9%	24 min	·OH, $·SO_4^{2-}$,$·O_2^-$	[3]
$CuFeO_2$/BC	Tetracycline	0.59 g/L, 57.63 mM H_2O_2, pH 6.27	89.12%	300 min	·OH	[4]
$CuFe_2O_4$/g-C_3N_4	Tetracycline	0.5 g/L, 10 mM H_2O_2, pH 5.37	93.6%	20 min	·OH, $·O_2^-$, $^1O_2$	[5]
Fe_2O_3/g-C_3N_4	Tetracycline	0.5 g/L, 10 mM H_2O_2, pH 6.2	90.7%	120 min	·OH, $·O_2^-$, h^+	[6]

References

[1] J.D.S. Salla, G.L. Dotto, D. Hotza, R. Landers, K.D.B. Martinello, E.L. Foletto. Enhanced catalytic performance of $CuFeS_2$ chalcogenide prepared by microwave-assisted route for photo-Fenton oxidation of emerging pollutant in water. *Journal of Environmental Chemical Engineering* 8 (2020) 1-10. https://doi.org/10.1016/j.jece.2020.104077

[2] J. Fang, F. He, Z. Yan, J. Wang, R. Yu, H. Zhou. Pyrite/biochar-activated peroxymonosulfate strengthens tetracycline degradation: important roles of surface functional groups and Fe(II)/Fe(III) redox cycling. *Journal of Environmental Chemical Engineering* 12 (2024) 112923. https://doi.org/10.1016/j.jece.2024.112923

[3] Y. Li, Y. Lu, X. Li, W. Zhong, B. Zhu, K. Liu. Enhanced activation of peroxymonosulfate for tetracycline degradation via cu-doped natural pyrite-based

$CuFeS_2$@FeS_2 composite catalysts: elucidating the catalytic mechanism and synergistic effect of dual catalytic sites. *Chem. Eng. J.* 509 (2025) 161454. https://doi.org/10.1016/j.cej.2025.161454

[4] S. Xin, G. Liu, X. Ma, J. Gong, B. Ma, Q. Yan, Q. Chen, D. Ma, G. Zhang, M. Gao, Y. Xin. High efficiency heterogeneous Fenton-like catalyst biochar modified $CuFeO_2$ for the degradation of tetracycline: economical synthesis, catalytic performance and mechanism. *Applied Catalysis B: Environmental* 280 (2021) 119386. https://doi.org/10.1016/j.apcatb.2020.119386

[5] G. Lu, L. Gou, M. Zhang, M. Guo. Enhanced antibiotic removal via cooperative reinforcement effect in (Cu,Mg)Fe_2O_4@g-C_3N_4 heterostructure: a multi-path generation of active species for rapid photo-Fenton-like catalysis. *J. Water Process. Eng.* 64 (2024) 105531 https://doi.org/10.1016/j.jwpe.2024.105531

[6] D. Meng, J. Hou, L. Wang, X. Hu, D. Gao, Q. Guo. Rational construction of α-Fe_2O_3@g-C_3N_4 heterojunction for effective photo-Fenton-like degradation of tetracycline. *Mater. Res. Bull.* 168 (2023) 112454. https://doi.org/10.1016/j.materresbull.2023.112454

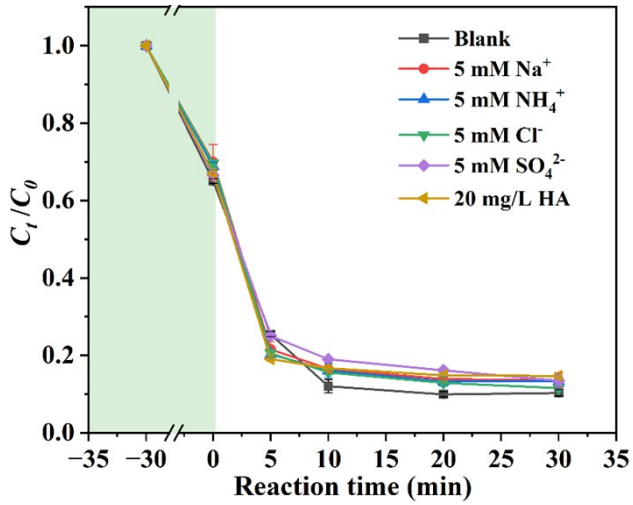

Fig. S2 Degradation curves of tetracycline in the presence of different cations, anions and humic acid. (Catalyst dosage 0.5 g/L, H_2O_2 concentration 3 mM, initial pH 5.92, cation concentration 5 mM, added as chlorides; anion concentration 5 mM, added as

sodium salts; humic acid concentration 20 mg·L^{-1})

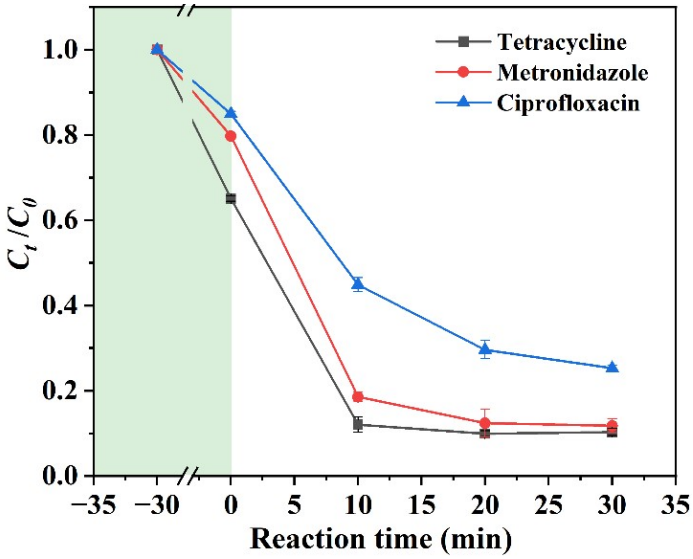

Fig. S3 Degradation profiles of different antibiotics catalyzed by copper sulfide. (Catalytic conditions: antibiotic concentration 20 mg·L^{-1}, catalyst dosage 0.5 g·L^{-1}, H_2O_2 3 mM)

Section S4. Detailed Process of Rietveld Refinement for the Phase Composition of Copper Sulfide Ore

4.1 Sample preparation

The copper sulfide ore samples were dried, then weighed and placed in an agate mortar for grinding. The final powder particle size was controlled to be less than 40 μm. All samples were subjected to XRD testing at room temperature (T = 298 K).

4.2 XRD instrument and testing conditions

The analysis was performed using a Rigaku D/Max-2500 X-ray diffractometer with a Cu Kα radiation source. The operating parameters were set as follows: voltage 40 kV, current 40 mA, scanning range 10°–70° (2θ), scanning speed 1°/min, and step size 0.02°. Data processing was performed using JADE Pro 9.1 software (International Centre for Diffraction Data - Materials Data, ICDD-MDI), with the ICDD 2024 PDF-5+ database. The following parameters were refined: zero shift, scale factors, unit cell parameters, peak profile parameters (U, V, W for the Caglioti function), and preferred orientation. Background was modeled using a 6th-order polynomial.

4.3. Sample testing

The ground sample was evenly spread in the sample holder, flattened with a glass slide, and then tested. XRD data were collected according to the aforementioned instrument parameters to obtain the diffraction pattern.

4.4 XRD Data analysis

4.4.1 Qualitative phase analysis

The diffraction pattern obtained from the experiment was analyzed using JADE Pro software. By comparing the 2θ peak positions in the experimental pattern with the standard diffraction data in the ICDD 2024 PDF-5+ database, phase matching was performed. The main phases identified in the pattern included: FeS_2 (PDF#98-000-0363) and $CuFeS_2$ (PDF#03-065-1573).

4.4.2 Quantitative phase analysis

(a) Data import: Import the experimentally obtained XRD data into JADE Pro software;

(b) Phase selection: Select the mineral phases involved in the fitting based on the qualitative analysis results;

(c) Crystal structure selection: To achieve quantitative analysis, choose known crystal structures as phase fitting models.

Table S2. Phase Composition, Phase Codes and Crystal Structure of Copper Sulfide Ore

Phase composition	Phase codes and crystal structure
FeS_2	98-000-0363, Cubic system
$CuFeS_2$	03-065-1573, Tetragonal system

(d) Model parameter initialization: The full-pattern fitting function initializes key parameters for each crystal structure, including zero-point shift, unit cell parameters, and intensity scaling factors.

(e) Rietveld automatic refinement process: The following lists the parameter changes of each crystal structure before and after Rietveld refinement to evaluate the refinement effect and model fitting quality.

Table S3. Refined and Unrefined Parameters of FeS_2

Parameter FeS_2	Zero shift value	Refined unit cell parameters	Intensity scaling factor	Temper-ature factor	Preferred orientation correction	Peak profile function	Full width at half maxima
Before refinement	0	a=5.418 b=5.418 c=5.418	36.1926	0	1.0	Pseudo-Voigt function	0.15392
After refinement	-0.04336	a=5.41902 b=5.41902 c=5.41902	41.3169	0	1.0	Pseudo-Voigt function	-0.01657

Table S4. Refined and Unrefined Parameters of $CuFeS_2$

Parameter $CuFeS_2$	Zero shift value	Refined unit cell parameters	Intensity scaling factor	Temper-ature factor	Preferred orientation correction	Peak profile function	Full width at half maxima
Before refinement	0	a=5.289 b=5.289 c=10.42	51.4675	0	1.0	Pseudo-Voigt function	0.17171
After refinement	-0.04336	a=5.29053 b=5.29053 c=10.42252	69.5979	0	1.0	Pseudo-Voigt function	0.03027

(f) Quantitative phase analysis: Upon completion of refinement, the JADE Pro software can automatically calculate the quantitative proportions of each phase.

(g) Precision evaluation: The weighted profile R-factor (Rwp) is a critical indicator for assessing the fitting quality of Rietveld refinement results, reflecting the consistency between the calculated and experimental diffraction patterns. Generally, when the Rwp value converges and falls below 15%, the refinement results can be considered reliable. During the whole-pattern fitting-Rietveld analysis of copper sulfide concentrate, after eliminating various Table S4. Rwp values for XRD refinement results interferences, the final obtained Rwp value was 5.01%, indicating high credibility of the fitting results.

Table S5. Rwp values for XRD Refinement Results

Substance	Rwp value
copper sulfide concentrate	5.01%

(h) Result analysis:

Using the JADE Pro software, quantitative analysis of copper sulfide ore was performed via whole-pattern fitting-Rietveld method. The results revealed its main phase composition as follows: FeS_2 accounted for 37.94% with an error of 1.14%, and

$CuFeS_2$ accounted for 62.06% with an error of 1.11%. When using JADE Pro software for XRD quantitative analysis, the result error is typically controlled within 10%, and all such errors fall within the standard error range permitted by the software, indicating that the analysis results possess good reliability.

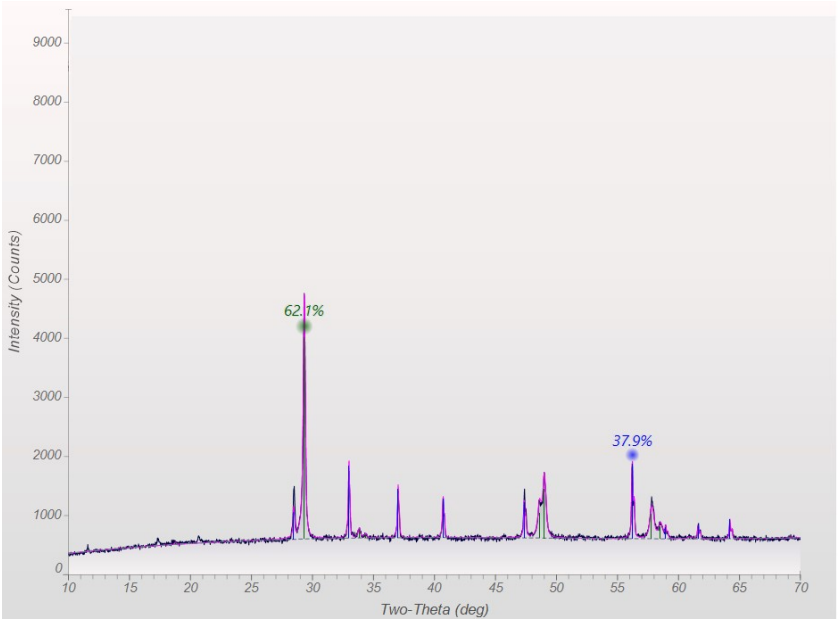

Fig. S4 Schematic diagram of the Rietveld refinement.

Phase ID (2)	Chemical Formula	PDF-#	Wt% (σ)	DD% (σ)	RIR	μ
Pyrite (?)	FeS_2	98-000-0363	37.94 (1.14)	43.27 (0.20)	3.00	956.3
Chalcopyrite	$CuFeS_2$	03-065-1573	62.06 (1.11)	56.73 (0.13)	7.47	598.2

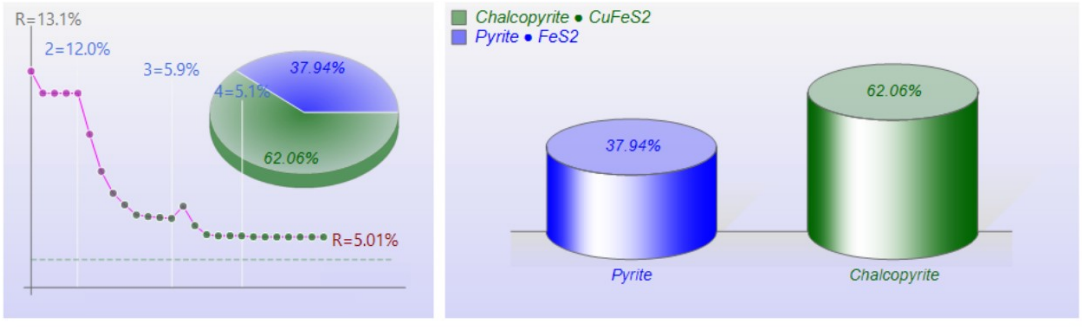

Fig. S5 Schematic diagram of the phase composition of the Rietveld refinement.

The final refinement converged with the following agreement indices:

Rwp (weighted profile R-factor) = 5.01%, Rp (profile R-factor) = 3.84%

χ^2 (goodness of fit) = 1.12, Fitting range: 10–70° 2θ

Number of refined parameters: 24, DWd (Durbin-Watson statistic) = 1.87

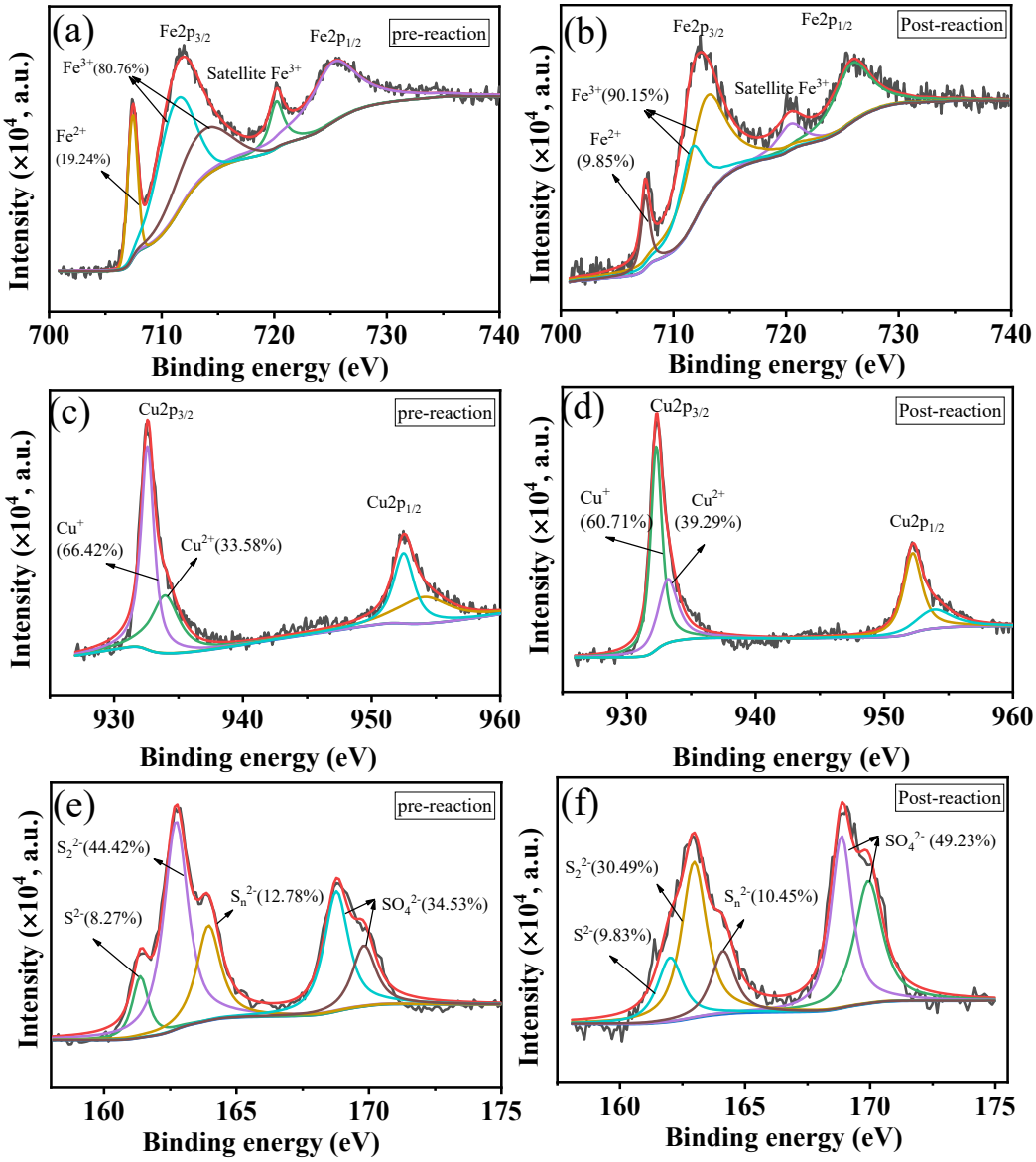

Fig. S6 XPS spectra of different elements in the catalyst before and after the reaction: (a-b) Fe, (c-d) Cu, (e-f) S.

Section S5. Leached Ion Concentrations in TC Solution

Table S6. Leached Ion Concentrations at Different Cycling Times

Cycling times	Ion concentration (mg/L)	
	Fe	Cu
1	5.783	27.327
2	2.479	10.767
3	1.583	4.582
4	0.584	2.313
5	0.270	2.241

Table S7. Leached Ion Concentrations in Different Reaction Time

Reaction time (min)	Ion concentration (mg/L)	
	Fe	Cu
2	1.137	5.357
6	2.752	15.354
10	5.144	25.983
30	5.783	27.328

Table S8. Tetracycline Identification of Intermediate Product Summary

	Reaction Time (min)	Accurate Mass $[M+H]^+$ (Da)	Theoretical mass [M+H]+ (Da)	Molecular Formula [M+H]+ (Da)	Proposed Structures
1	21.1	461.1284	461.1482	$C_{22}H_{25}N_2O_8$	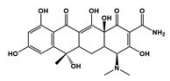
2	2.8	475.121	475.1274	$C_{22}H_{23}N_2O_{10}$	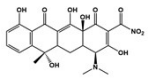
3	20.5	417.3657	417.1584	$C_{22}H_{23}N_2O_7$	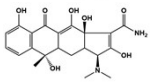
4	20.5	433.1054	433.1533	$C_{21}H_{25}N_2O_8$	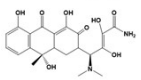
5	21.1	459.1082	459.1325	$C_{22}H_{23}N_2O_9$	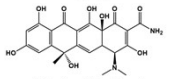
6	19.6	477.1732	477.1431	$C_{22}H_{25}N_2O_{10}$